Denervation-induced skeletal muscle fibrosis is mediated by CTGF/CCN2 independently of TGF-β

Daniela L. Rebolledo[a,d], **David González**[a,b], **Jennifer Faundez-Contreras**[a,b], **Osvaldo Contreras**[a,b], **Carlos P. Vio**[a,c], **Joanne E. Murphy-Ullrich**[e], **Kenneth E. Lipson**[f] **and Enrique Brandan**[a,b]

a - Centro de Envejecimiento y Regeneración, *CARE Chile UC, Chile*
b - Departamento de Biología Celular y Molecular, *Chile*
c - Departamento de Ciencias Fisiológicas, *Facultad de Ciencias Biológicas, Pontificia Universidad Católica de Chile, Santiago, Chile*
d - Escuela de Obstetricia y Puericultura, *Facultad de Salud, Universidad Bernardo O Higgins, Santiago, Chile*
e - Departments of Pathology, *Cell Developmental and Integrative Biology, and Ophthalmology, The University of Alabama at Birmingham, AL, USA.*
f - FibroGen Inc., *San Francisco, CA, USA*

Correspondence to Enrique Brandan: *Pontificia Universidad Católica de Chile, Libertador Bernardo O'Higgins 340, Code Postal 8331150 Santiago, Chile.* *drebolledo@bio.puc.cl*
https://doi.org/10.1016/j.matbio.2019.01.002

Abstract

Muscular fibrosis is caused by excessive accumulation of extracellular matrix (ECM) that replaces functional tissue, and it is a feature of several myopathies and neuropathies. Knowledge of the biology and regulation of pro-fibrotic factors is critical for the development of new therapeutic strategies. Upon unilateral sciatic nerve transection, we observed accumulation of ECM proteins such as collagen and fibronectin in the denervated hindlimb, together with increased levels of the profibrotic factors transforming growth factor type β (TGF-β) and connective tissue growth factor (CTGF/CCN2). In mice hemizygous for CTGF/CCN2 or in mice treated with a blocking antibody against CTGF/CCN2, we observed reduced accumulation of ECM proteins after denervation as compared to control mice, with no changes in fibro/adipogenic progenitors (FAPs), suggesting a direct role of CTGF/CCN2 on denervation-induced fibrosis. During time course experiments, we observed that ECM proteins and CTGF/CCN2 levels are increased early after denervation (2–4 days), while TGF-β signaling shows a delayed kinetics of appearance (1–2 weeks). Furthermore, blockade of TGF-β signaling does not decrease fibronectin or CTGF levels after 4 days of denervation. These results suggest that in our model CTGF/CCN2 is not up-regulated by canonical TGF-β signaling early after denervation and that other factors are likely involved in the early fibrotic response following skeletal muscle denervation.

Introduction

After acute damage, most tissues undergo a series of events that remove damaged structures and replace them with new functional cells. Under chronic damage, the affected tissue cannot be completely repaired, producing an imbalance that leads to excessive production and accumulation of extracellular matrix (ECM) proteins such as proteoglycans, fibronectin and different types of collagens, which surround the cells of the affected tissue [1–3]. This phenomenon, called fibrosis, is a hallmark of several chronic pathologies affecting almost every organ [4], including myopathies as muscular dystrophies, where scar-like tissue replaces functional cells and creates a physical barrier that inhibits regeneration, neovascularization, and the possibility of successful cell therapy [5–8].

Skeletal muscle denervation is the interruption of synaptic transmission from motoneurons to their skeletal muscle targets. It can occur as a consequence of trauma or pathological conditions: transection of

the nerve, death of motoneurons as in neurodegenerative diseases like Amyotrophic Lateral Sclerosis (ALS) [9], loss of acetylcholine receptors (AChRs) in diseases such as Myasthenia gravis [10], and during aging [11]. Transection of the sciatic nerve and blockade of nerve transmission have been largely used as experimental approaches [12–14]. Skeletal muscle alterations after denervation are numerous, including atrophy and increased autophagy [15,16], inflammation [17], AChR degradation [18], changes in gene expression profile [19], alterations in mitochondrial function [20] and delocalization of neuronal nitric oxide synthase μ from the sarcolemma [21]. Increases in ECM components and fibrotic markers have also been described after denervation [12,14,22–25]. Furthermore, fibro/adipogenic progenitors (FAPs), skeletal muscle resident cells that differentiate to myofibroblasts producing ECM and are involved in the fibrotic response, are also augmented after denervation [26] and in a murine ALS model [27,28].

Connective tissue growth factor (CTGF/CCN2) is a matricellular protein that is expressed at very low levels in adulthood but its levels increase in challenged tissues, for example under pathological conditions [29,30]. CTGF/CCN2 is increased in muscular dystrophies [31] and in the *mdx* mouse, a murine model for Duchenne Muscular Dystrophy [32,33], as well in the tg-hSOD^{G93A} mouse model for ALS [27,34]. CTGF/CCN2 is a strong profibrotic factor that colocalizes with fibrotic and necrotic/regenerative foci in damaged muscle [35,36] and promotes fibroblast proliferation and ECM production by several different cell types, both in vitro and in vivo [29,37–40]. Through experiments of gain and loss of CTGF/CCN2 function, our laboratory showed that CTGF/CCN2 plays a critical role in promoting fibrosis: overexpression of CTGF/CCN2 in healthy wild type skeletal muscle is sufficient to induce a fibrotic phenotype with a reduction of skeletal muscle strength [39], whereas decreased CTGF/CCN2 levels or activity reduces muscle damage, fibrosis, muscle weakness and can improve cell therapy [32,34].

Transforming growth factor type β (TGF-β) has been extensively studied and linked to fibrosis associated with different pathologies [24,41–43] including muscular dystrophies [44,45]. The canonical TGF-β or Smad-dependent pathway involves phosphorylation of Smad2/3 directly by the TGF-β receptor I kinase (TGF-βRI), binding to Smad4 and translocation of this complex into the nucleus to drive the expression of target genes that contribute to the fibrotic process, including induction of CTGF/CCN2 [29,40,41,46–48]. Increased TGF-β signaling after denervation or inhibition of electric activity has been reported previously [13,23,26]. Furthermore, it has been shown increased TGF-β signaling and CTGF/CCN2 levels in an ALS model during symptomatic stages, when muscle innervation is already compromised [27,34,49,50]. However, whether TGF-β induces CTGF/CCN2 after denervation and if CTGF/CCN2 has a role in denervation-induced fibrosis, are questions that have not yet been explored.

In this work, we show that denervation-induced fibrosis is accompanied by increased TGF-β signaling and CTGF/CCN2 expression. We found that reduction of CTGF/CCN2 levels using a genetic model or inhibition of CTGF/CCN2 activity with a monoclonal anti-CTGF/CCN2 antibody decreased ECM accumulation, suggesting that CTGF/CCN2 also has a role in fibrosis upon denervation. Interestingly, the decreased fibrosis in the CTGF/CCN2 inhibition models is not due to FAPs reduction. Furthermore, through kinetic experiments in these models and by the use of TGF-β inhibitors, we show that the induction of CTGF/CCN2 occurs early after denervation, independent of TGF-β signaling. Thus, early CTGF/CCN2 and ECM stimulation in this model occur through a TGF-β independent mechanism.

Results

Denervation-induced skeletal muscle fibrosis is accompanied by increased TGF-β and CTGF/CCN2 levels

To evaluate the role of TGF-β and CTGF/CCN2 in the fibrotic process induced after denervation, we performed unilateral sciatic nerve transection in 6–8-month old C57BL10 wild type mice and

Fig. 1. Accumulation of skeletal muscle ECM proteins and increased levels of the profibrotic factors TGF-β and CTGF/CCN2 two weeks after denervation. 6–7-month-old C57BL10 mice were subjected to unilateral sciatic denervation and skeletal muscle from both hindlimbs were collected 2 weeks after denervation. A. Frozen tissue cross-sections from contralateral and denervated muscles were stained with H&E, Sirius Red (total Collagen) and subjected to IFI for detection of fibronectin and Collagen I. Bar, 100 μm. B. TGF-β1 mRNA levels were measured by quantitative RT-PCR. N = 8. C. Fluorescent immunostaining (IFI) against pSmad3 and laminin in denervated muscles when compared to contralateral muscles. N = 4. Bar, 50 μm. D. Quantification of total pSmad3 positive nuclei in denervated muscles when compared to contralateral muscles. N = 4. E. Quantification of pSmad3 positive nuclei in muscle fibers and interstitial cells from control and denervated muscle. N = 3. F. IFI against pSmad3 in control and denervated muscle from mice expressing EGFP in PDGFRα positive cells, as a marker of FAPs. Bar, 50 μm. G. IHC against CTGF in control and denervated muscle. H. Quantification of CTGF occupied area in control and denervated muscles. Bar: 100 μm. I. Representative WB in muscle lysates for CTGF show increased CTGF levels upon denervation. J. Densitometric quantification from WB in I. N = 7 mice.

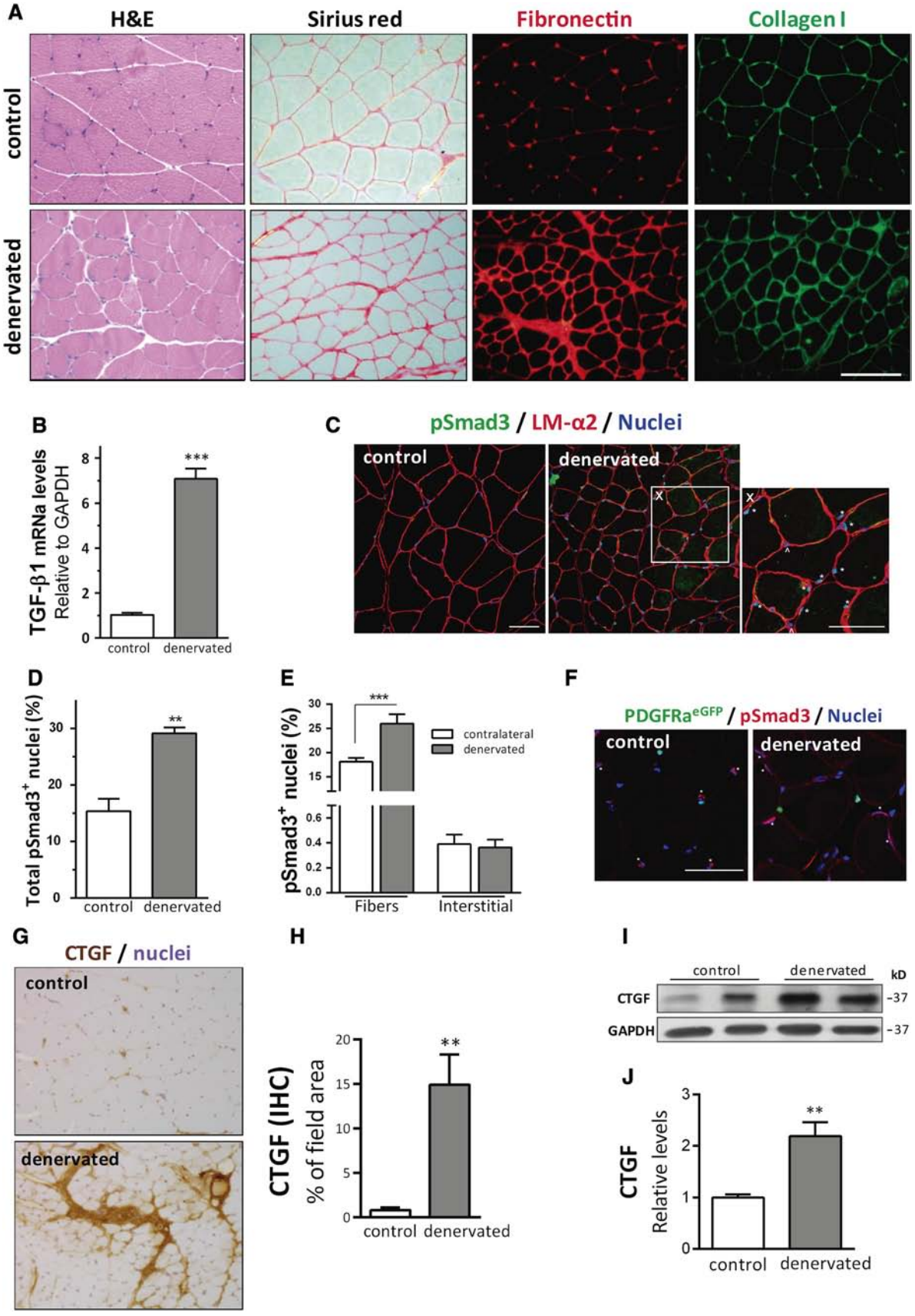
A
H&E
Sirius red
Fibronectin
Collagen I
control
denervated
B
TGF-β1 mRNA levels
Relative to GAPDH
***
control
denervated
C
pSmad3 / LM-α2 / Nuclei
control
denervated
D
Total pSmad3+ nuclei (%)
**
control
denervated
E
pSmad3+ nuclei (%)
***
contralateral
denervated
Fibers
Interstitial
F
PDGFRaeGFP / pSmad3 / Nuclei
control
denervated
G
CTGF / nuclei
control
denervated
H
CTGF (IHC)
% of field area
**
control
denervated
I
control
denervated
kD
CTGF
GAPDH
-37
-37
J
CTGF
Relative levels
**
control
denervated

compared changes between the denervated hindlimb and the non-denervated (contralateral) internal control. Two weeks after denervation we observed an evident increment in the interstitial space as well as the already described muscle atrophy [15] (Fig. 1A). We used sirius red staining and indirect immunofluorescence (IFI) to evaluate levels of ECM proteins. When compared to contralateral non-denervated gastrocnemius (GT), denervated muscles showed augmented deposition of total collagen, collagen I and fibronectin (Fig. 1A), indicating an increase in skeletal muscle fibrosis as a consequence of denervation, which confirmed previous reports [12,24,26]. These changes were also observed in other muscles such as tibialis anterior (TA) and flexor digitorius brevis (data not shown).

Because the role of TGF-β signaling in skeletal muscle fibrosis is well described [45], we evaluated whether this signaling pathway also participates in denervation-induced fibrosis. We observed that after 2 weeks of sciatic nerve section TGF-β1 mRNA levels (Fig. 1B) and the total number of positive nuclei for effector pSmad3 were increased in denervated GT (Fig. 1C–D), indicating the activation of canonical TGF-β signaling in denervated muscles. Given the high diversity of skeletal muscle cell types, we aimed to determine which cells were activating Smad-dependent TGF-β signaling. Then, we used laminin immune staining to outline muscle fibers, and *Pdgfrα*$^{tm11(EGFP)Sor}$ mice to discriminate PDGFRα expressing FAPs by localizing nuclear EGFP fluorescence [51]. Interestingly, we observed that the increment in pSmad3 positive nuclei after denervation correspond mostly to nuclei of myofibers and not from interstitial cells (Fig. 1E) and do not colocalize with EGFP expressing FAPs (Fig. 1F).

Since the expression of CTGF/CCN2 is induced by TGF-β, we aimed to determine whether CTGF/CCN2 was upregulated after denervation. We observed that CTGF/CCN2 levels were increased in denervated muscles after 2 weeks as compared to contralateral controls (Fig. 1G–J) when evaluated by western blot (WB) and immunohistochemistry (IHC), suggesting a role for CTGF/CCN2 in developing denervation-induced fibrosis. These results indicate that after denervation of skeletal muscle there is an important increase in pro-fibrotic factors and ECM proteins.

Mice with decreased CTGF/CCN2 levels or activity show less skeletal muscle ECM accumulation after 2 weeks of denervation

In order to evaluate whether CTGF/CCN2 has a role in developing fibrosis upon denervation, we used two different strategies to decrease CTGF/CCN2 levels or activity. First, we performed sciatic nerve transection in mice hemizygous for the Ctgf/Ccn2 gene (Ctgf/Ccn2$^{+/-}$), which produce reduced levels of CTGF/CCN2 protein [32,52]. As second approach, we used FG-3019 (FibroGen Inc.), a human monoclonal antibody that blocks CTGF/CCN2 activity [32,34]. This strategy allowed us to neutralize CTGF/CCN2 activity just prior to performing the sciatic nerve transection, whereas reduced levels of CTGF/CCN2 in Ctgf/Ccn2$^{+/-}$ mice were sustained from developmental stages. Thus, wild type C57BL10 mice were systemically treated with IP FG-3019 injections (FibroGen, USA) or control human IgG (h-IgG), for 3 weeks. After 1 week of treatment, mice were unilaterally denervated, and their muscles collected for analysis 2 weeks later. Two weeks after denervation we observed less muscular fibronectin and total collagen deposition in Ctgf/Ccn2$^{+/-}$ mice as compared to Ctgf/Ccn2$^{+/+}$ littermates (Fig. 2A, C). We also observed less accumulation of fibronectin and collagen I upon denervation in muscle sections from mice treated with FG-3019, compared to h-IgG-treated animals (Fig. 2B, D). Lower abundance of fibronectin was also observed when we analyzed whole muscle extracts of GT by WB: the amount of fibronectin in denervated muscle from Ctgf/Ccn2$^{+/-}$ mice is lower than in wild type mice (Fig. 3A) and in FG-3019-treated mice compared to controls (Fig. 3B). Denervation increased CTGF/CCN2 levels as showed above, but a lower amount of CTGF/CCN2 is observed in muscles from Ctgf/Ccn2$^{+/-}$ mice compared Ctgf/Ccn2$^{+/+}$ animals when denervated. In contrast, CTGF/CCN2 levels remain the same in treated and control mice, since the antibody blocks CTGF/CCN2 activity without necessarily decreasing its levels [34]. Nevertheless, TGF-β signaling, determined by total TGF-β1 mRNA levels and percent of pSmad3 positive nuclei, remained increased in denervated GT from both Ctgf/Ccn2 hemizygous mice and FG-3019-treated mice (Fig. 3C–H). As control for FG-3019 treatment, we used a fluorophore (Alexa-568) labeled anti-human antibody in IFI and were able to detect the presence of treatment antibodies in muscle cryosections, indicating that FG-3019 and control h-IgG reached the target tissue. Also, the FG-3019 anti-CTGF/CCN2 antibodies are more abundant in the tissue only in denervated muscle, where CTGF/CCN2 is elevated (Supplementary Fig. 1). Furthermore, skeletal muscle sequential cross-sections from denervated mice treated with FG-3019 shows that anti-CTGF staining colocalizes with FG-3019 accumulation in the tissue, detected by the anti-human antibody, indicating the efficacy of FG-3019 in binding CTGF (Fig. 3I). Altogether, these results strongly suggest that CTGF/CCN2 has a direct role in denervation-induced fibrosis in skeletal muscle and that blocking CTGF/CCN2 decreases the accumulation of ECM proteins after denervation. Our laboratory has already shown that inhibition of CTGF/CCN2 reduces fibrosis but also enhances skeletal muscle strength in *mdx* mice [32] and in the hSOD1^{G93A}

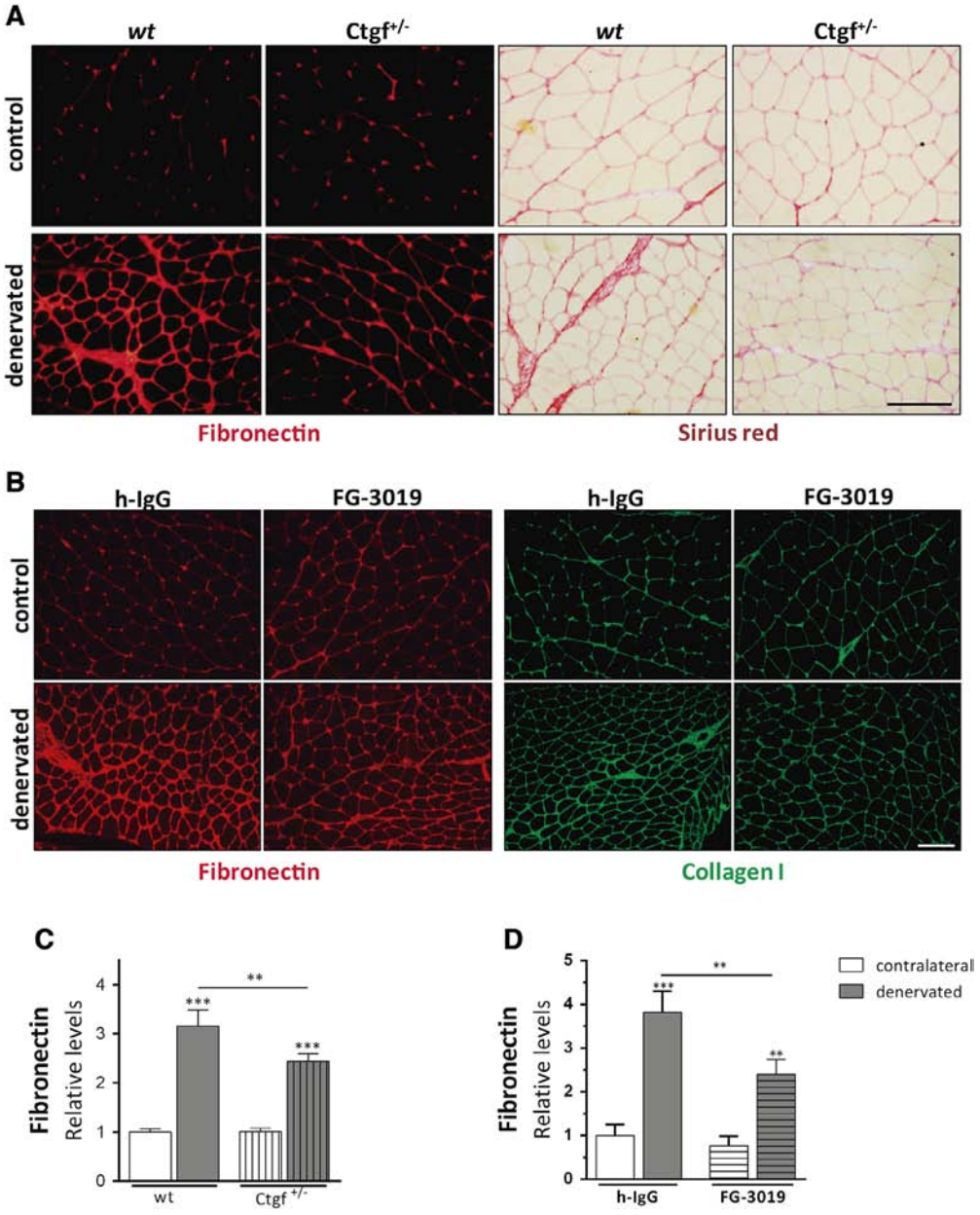

Fig. 2. Mice with decreased CTGF/CCN2 levels or activity present reduced skeletal muscle ECM accumulation 2 weeks after denervation. A. Mice hemizygous for the Ctgf gene ($Ctgf^{+/-}$, N = 7) and their *wt* littermates ($Ctgf^{+/+}$, N = 10) were subjected to unilateral sciatic denervation and skeletal muscles from both hindlimbs were collected 2 weeks after the procedure. IFI against fibronectin and Sirius red staining for total collagen show less accumulation of these ECM proteins upon denervation in $Ctgf^{+/-}$ mice as compared to control littermates. Bar: 100 μm B. C57Bl10 mice were systemically treated with anti-CTGF-blocking antibody (FG-3019, N = 10) or control h-IgG (N = 7), and unilaterally denervated. Muscles were analyzed 2 weeks after denervation. IFI against fibronectin and collagen I show that mice treated with FG-3019 have less accumulation of ECM proteins when denervated compared to mice treated with h-IgG. Bar: 100 μm. C–D. Quantification of the area occupied by fibronectin measured from IFI microphotographs.

mouse, a model for ALS [34]. Here, we observed that reduced isometric force in isolated denervated TA muscle and muscle fiber atrophy was not improved in $Ctgf/Ccn2^{+/-}$ or FG-3019-treated mice (Supplementary Fig. 2), suggesting that the effects of decreasing CTGF/CCN2 are related to muscle fibrosis and not muscle force and atrophy under full denervation conditions for 2 weeks.

FAPs expressing PDGFR-α and Tcf4 are increased in denervated skeletal muscle [26]. To evaluate if

CTGF has a role in regulating the amount of FAPs, we used total homogenates from control and denervated muscles for 2 weeks and evaluated PDGFR-α and Tcf4 levels. As shown before, denervation increases FAPs markers compared to contralateral hindlimbs, however, the increment on PDGFR-α and Tcf4 observed after denervation is not changed by FG-3019 treatment (Fig. 3J) or in Ctgf/Ccn2 hemizygous mice (Supplementary Fig. 3). These results suggest that the reduction in denervation-induced fibrosis

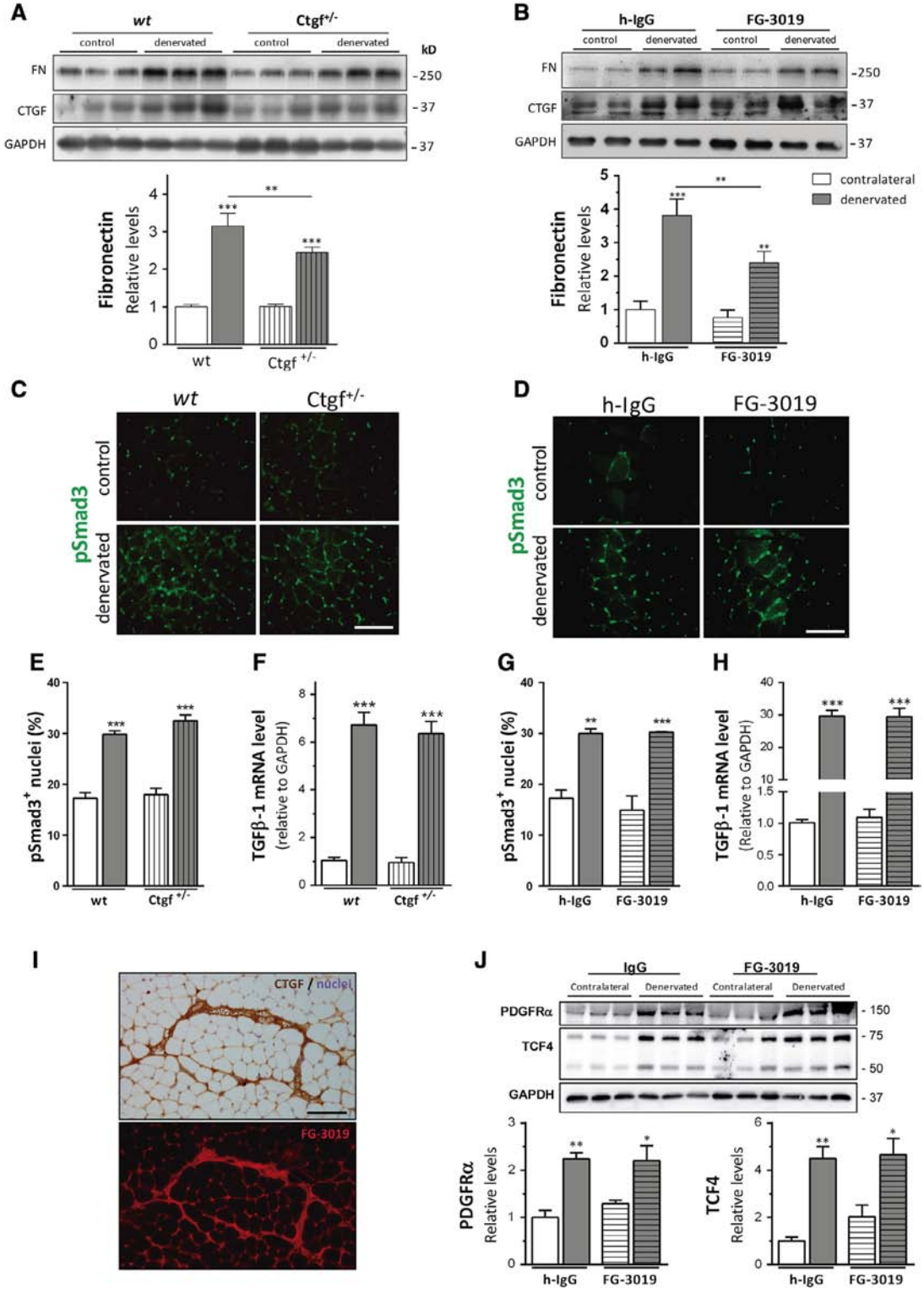

observed in CTGF/CCN2 inhibition models is not related to reduction in FAPs.

Skeletal muscle ECM accumulates and CTGF/CCN2 levels increase early after denervation independently of TGF-β signaling

To evaluate the kinetics of the denervation-related fibrotic response, we performed time course experiments, to evaluate muscles after 2, 4, 7 and 14 days of unilateral sciatic nerve transection. IFI experiments show that ECM proteins such as fibronectin and collagen I are increased early after denervation, as soon as 2 days post sciatic nerve transection (Fig. 4). Increased fibronectin was also confirmed by WB analyses of muscle homogenates obtained at the indicated days (Fig. 5A–B). In the same samples, we observed that CTGF/CCN2 protein levels, evaluated by WB, were also elevated since 2 days after denervation (Fig. 5A–B). Elevated CTGF/CCN2 protein levels 2 days after denervation were more variable than other time points, then not statistically significant. Then, CTGF/CCN2 levels were also evaluated by IHC in muscle cryosections (Fig. 5C–D), ratifying increased protein levels since 2 days after denervation. These results suggest an early role for CTGF/CCN2 in the induction of skeletal muscle fibrosis after denervation. Interestingly, we observed that TGF-β1 mRNA also increases after denervation but at later times and with a slightly delayed expression kinetics compared to increased CTGF/CCN2 levels (Fig. 5E), as we previously showed [26]. Furthermore, the number of positive nuclei for the downstream canonical effector pSmad3 remains unchanged 2 and 4 days after denervation and only appears significantly elevated 2 weeks after denervation (Fig. 5E), while TGF-$\alpha_{1,2,3}$ detected by WB increased with time after denervation with no statistical significance due to high variability between samples (Fig. 5F). These results suggest that the induction of skeletal muscle CTGF/CCN2 levels upon denervation occurs before the activation of canonical TGF-β signaling and might be independent of it.

In order to evaluate whether TGF-β signaling is required for the early induction of CTGF/CCN2, we treated mice with SB525334, an inhibitor of TGF-β receptor I (TGF-β-RI) kinase, and evaluated the levels of CTGF/CCN2 and fibronectin 4 days after denervation. We observed that CTGF/CCN2 and fibronectin levels were increased 4 days after denervation despite TGF-β-RI inhibition, and at similar levels as in vehicle-treated mice (Fig. 6A–C). We performed the same experiment with a different TGF-β-RI kinase inhibitor, SB431542, and observed the same response (Supplementary Fig. 4). To further reinforce this observation, we used a different approach to block TGF-β signaling using SRI31277, an inhibitor of thrombospondin 1 (TSP1) [53]. TPS1 regulates the release of latent TGF-β from insulted tissue and SRI31277 has been shown to block TGF-β signaling in different models [53–57]. We observed that treatment with SRI31277 was unable to reduce skeletal muscle CTGF/CCN2 and ECM accumulation 4 days after denervation (Fig. 6D–F), similar to what we observed when blocking TGF-β-RI kinase activity. This lack of effect was not due to inactivity of these inhibitors in this model as there was a decrease in pSmad3 immunostaining in animal treated with either the TGF-βRI kinase inhibitors or the TSP1 antagonist (Fig. 6G–H and Supplementary Fig. 4).

CTGF/CCN2 is required for induction of skeletal muscle ECM proteins early after denervation

Since we observed that skeletal muscle accumulation of ECM proteins 2 weeks after denervation was reduced when CTGF/CCN2 levels or activity were blocked (Figs. 2 and 3), we decided to evaluate whether CTGF/CCN2 is actually required for ECM expression early after denervation. We used either Ctgf/Ccn2$^{+/-}$ or wild type (*wt*) mice treated with FG-3019 blocking antibody against CTGF/CCN2 and evaluated the muscles 4 days after sciatic nerve unilateral denervation. We observed that the increase in fibronectin was decreased in both Ctgf/Ccn2$^{+/-}$ and FG-3019 treated mice compared to controls (Fig. 7A–D). Altogether, these results indicate that skeletal muscle CTGF/CCN2 was induced early after denervation (2–4 days) and that CTGF/CCN2 was required for the observed accumulation of ECM. However, our results suggest that the early induction of CTGF/CCN2 is not dependent on canonical TGF-β signaling.

Fig. 3. Mice with decreased CTGF/CCN2 levels or activity present reduced skeletal muscle ECM accumulation after 2 weeks of denervation without changes in TGF-β signaling. A–B. Muscle homogenates from Ctgf hemizygous mice (A) and mice treated with FG-3019 (B) and their corresponding controls were subjected to SDS-page and immunoblotted for fibronectin and CTGF. At the bottom, fibronectin levels were quantified by densitometric analysis. N = 7 for *wt* and N = 10 for Ctgf$^{+/-}$ mice. N = 7 for h-IgG and N = 10 for FG-3019 treated mice. C–D Total pSmad3 positive nuclei were evaluated by IFI and quantified in E and G, calculating the percentage of total nuclei in the field, considering at least 6 different fields per muscle, from 3 mice for every condition. Bar: 100 μm. F and H. TGF-β1 mRNA levels were also evaluated in CTGF hemizygous mice (N = 5 for *wt* and N = 5 for Ctgf$^{+/-}$) and FG-3019 treated mice (N = 3 for h-IgG, N = 5 for FG-3019). I. IHC against CTGF and IFI against hu-IgG performed in denervated muscle cross-section from FG-3019 treated mice. J. WB against PDGFRα and Tcf4 as markers of FAPs in denervated muscle from h-IgG and FG-3019 treated mice, quantified at the bottom. In all graphs, white bars correspond to contralateral hindlimbs and gray bars to denervated hindlimbs. (N = 3 for each condition).

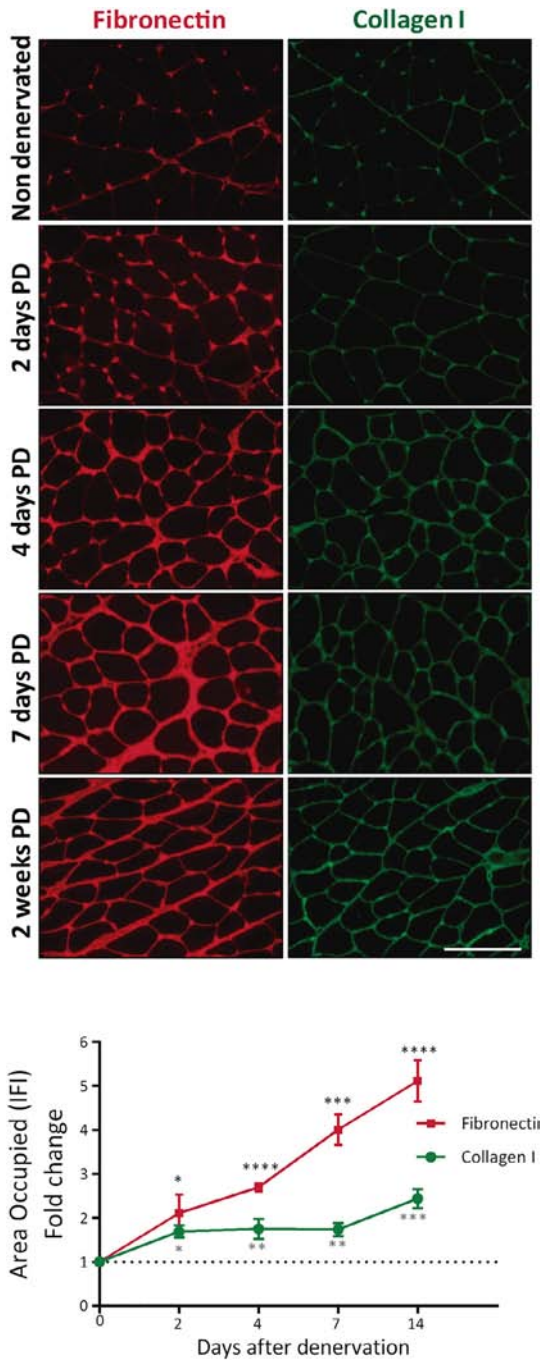

Fig. 4. Skeletal muscle ECM proteins increase early after denervation. 6–7-month-old C57Bl10 mice were subjected to unilateral sciatic denervation and euthanized 2 days, 4 days, 7 days or 2 weeks after denervation. Immunostaining for fibronectin and collagen I show that ECM accumulation starts early after denervation and accumulates in later stages, which is quantified in the graph below. Contralateral levels of fibronectin and collagen I (control) remained unaltered independently of the time of denervation (data not shown). Bar = 100 μm.

Discussion

Fibrosis is the final outcome of most chronic, inflammatory and autoimmune pathologies affecting almost every organ and accounting for approximately 40% of deaths in developed countries [4,42]. Consequently, knowledge of the physiology and the cellular and molecular basis of the fibrotic process will open possibilities for new therapeutic alternatives to be used in patients suffering fibrotic diseases of diverse etiology. Changes in tissue remodeling and increased accumulation of ECM proteins after denervation have been described by different groups. Despite differences in the animal models used (rat vs mouse, for example), type of damage and muscles evaluated, a common feature is the accumulation of ECM proteins associated with enhanced TGF-β expression and changes in metalloprotease activity [24,58,59]. To date, several molecules involved in the skeletal muscle fibrotic response have been studied by us and others. The data shows that the inhibition of pro-fibrotic factors or the activation of anti-fibrotic pathways can reduce fibrosis, resulting in improved structure, perfusion, and tissue function [2,7,8,60,61]. In this respect, our laboratory has been interested in studying the biology and pro fibrotic effects of CTGF/CCN2 in skeletal muscle fibrotic disease. Here, we report that skeletal muscle fibrosis induced by sciatic denervation associates with increased TGF-β signaling and CTGF/CCN2 expression. Liu et al., previously reported that denervation of the sternocleidomastoid muscle was accompanied by increased TGF-β and CTGF/CCN2 levels 1 week after denervation [58]. Also, increased Smad2/3 proteins after 1 week of denervation has been reported and showed to be required for denervation-induced protein degradation and atrophy [62]. However, earlier times were not evaluated, and neither was the effect of inhibition of either of the profibrotic factors.

In this work, we propose a role for CTGF/CCN2 in denervation-induced fibrosis since we observed a decrease in ECM proteins accumulation when CTGF/CCN2 levels (in hemizygous mice) or activity (using the FG-3019 antibody) were reduced. The reduction of skeletal muscle fibrosis as a consequence of CTGF/CCN2 inhibition not only recounts what had been reported on fibrosis related to dystrophic *mdx* muscle [32], but also to what we observed in the hSOD1^{G93A} transgenic mouse model of ALS [34]. Interestingly, here we show that under conditions where CTGF/CCN2 is inhibited, the augmented number of FAPs after denervation were not affected, suggesting that CTGF/CCN2 is not influencing the increase in FAPs. In the ALS model [34], fibrosis and skeletal muscle CTGF/CCN2 increased only in the symptomatic stages, when there were already signs of muscle denervation. This observation opened the question of whether muscle fibrosis is due to overexpression of mutant SOD1 or a

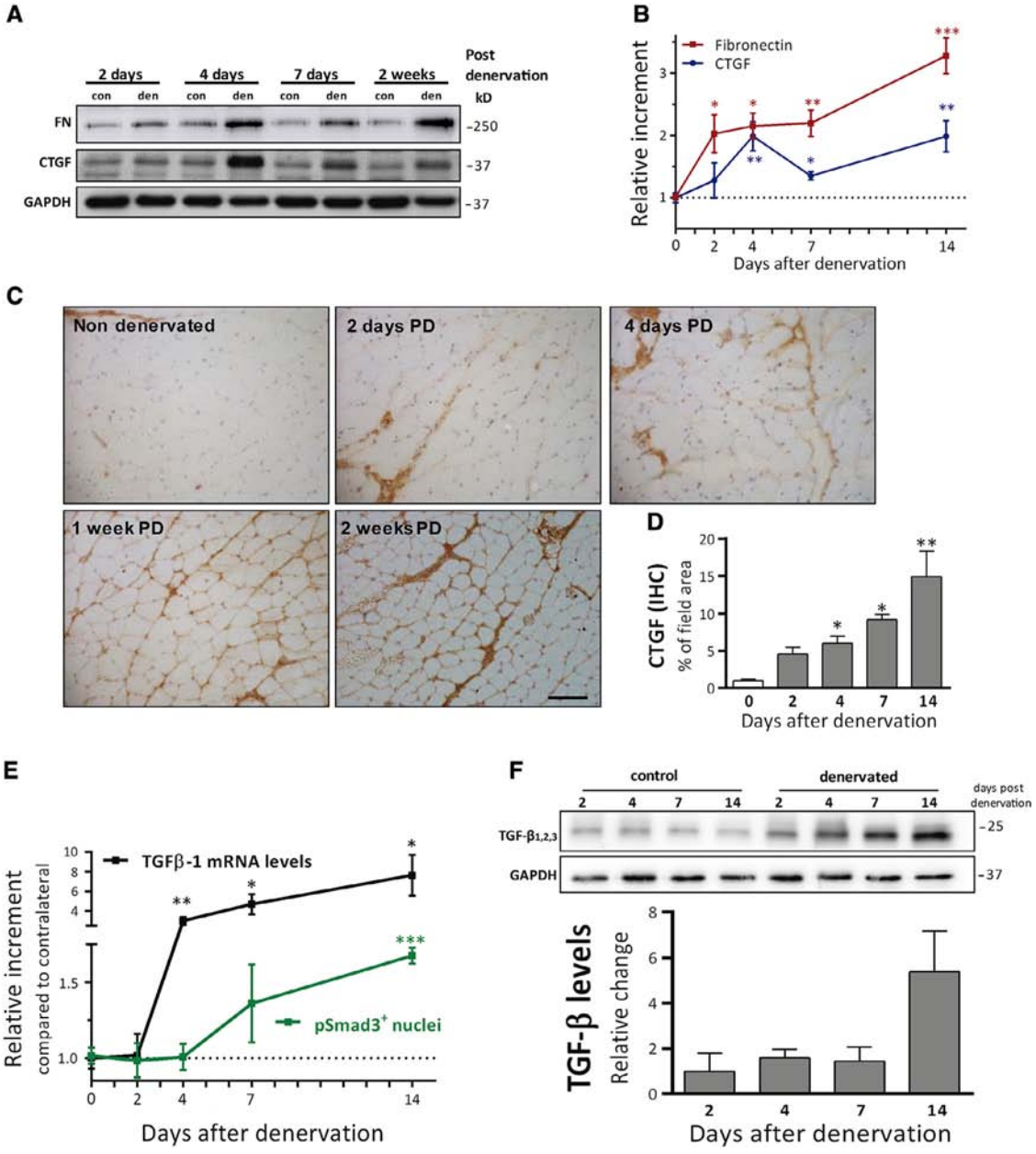

Fig. 5. Skeletal muscle CTGF/CCN2 levels increase earlier than TGF-β signaling after denervation. A. Muscle homogenates from mice collected 2, 4, 7 and 14 days after denervation were evaluated for fibronectin and CTGF. Along with an early increment of fibronectin after denervation, profibrotic CTGF is rapidly elevated. B. Densitometric analysis from 3 WB (N = 3 mice for each time point). C. CTGF immunostaining in frozen tissue sections shows the rapid increment in CTGF levels. CTGF area in cross-sectional areas is quantified in D Bar: 100 μm. E. TGF-β1 mRNA levels, measured by q-RT-PCR, do not rise until 4 days post denervation, while pSmad3 positive nuclei, quantified from IFI images, are not significantly incremented until 2 weeks after denervation. F. Representative WB against TGF-$\beta_{1,2,3}$ in denervation temporal course. Quantification is shown at the bottom (N = 3 mice for each time point).

consequence of muscle denervation. The inhibition of CTGF/CCN2 in the ALS model reduces skeletal muscle fibrosis but also improves muscle strength and locomotory function [34]. This might be explained because in this model, CTGF/CCN2 is also increased in the spinal cord in pre-symptomatic stages, and the inhibition of CTGF/CCN2 preserved nerve and neuromuscular junction integrity, decreasing denervation, and also showing an effect in the central nervous system. Here, we show that under conditions

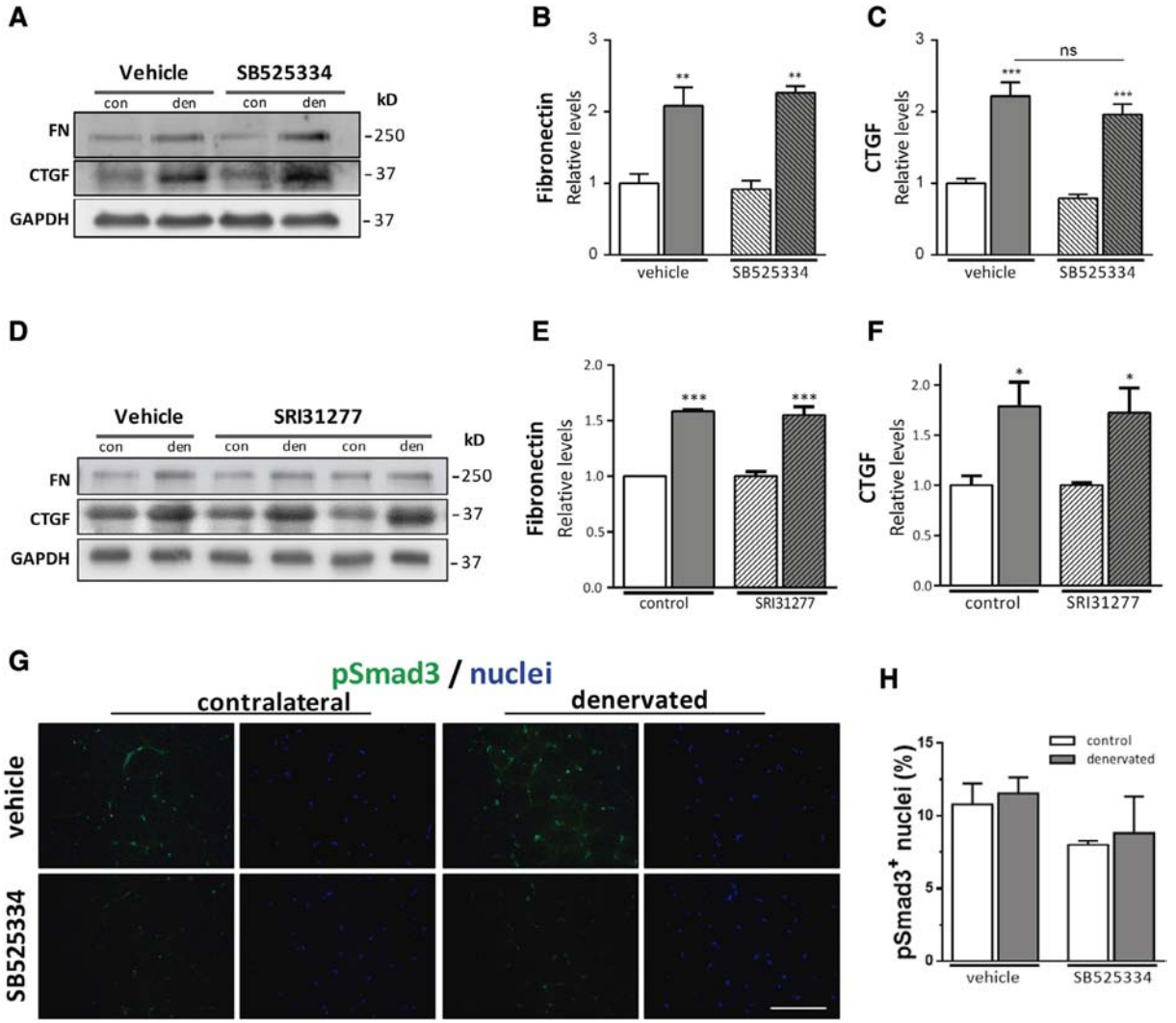

Fig. 6. Blockade of TGF-β signaling or activation does not affect the induction of skeletal muscle CTGF/CCN2 and fibronectin 4 days after denervation. A. Mice were treated with vehicle (DMSO) (N = 3) or SB525334 (N = 3) and muscles collected for analysis 4 days after denervation. WB analyses show that, despite TGF-β signaling inhibition, CTGF and Fibronectin protein levels increased similarly after denervation. B–C: The densitometric analysis of WB is shown to the right of a representative WB image. D. Mice were treated with vehicle (N = 3) or the TSP1 antagonist SRI31277 (N = 3) and muscles collected for analysis 4 days after denervation. WB analyses show that, despite inhibiting activation of latent TGF-β, CTGF and Fibronectin protein levels increase similarly after denervation. E–F: Densitometric analysis is shown to the right of a representative WB image. In all graphs, white bars correspond to contralateral hindlimbs and gray bars to denervated hindlimbs. G–H. IFI against pSmad3 was assessed to determine whether treatments were effective in blocking TGF-β signaling. Bar: 100 μm.

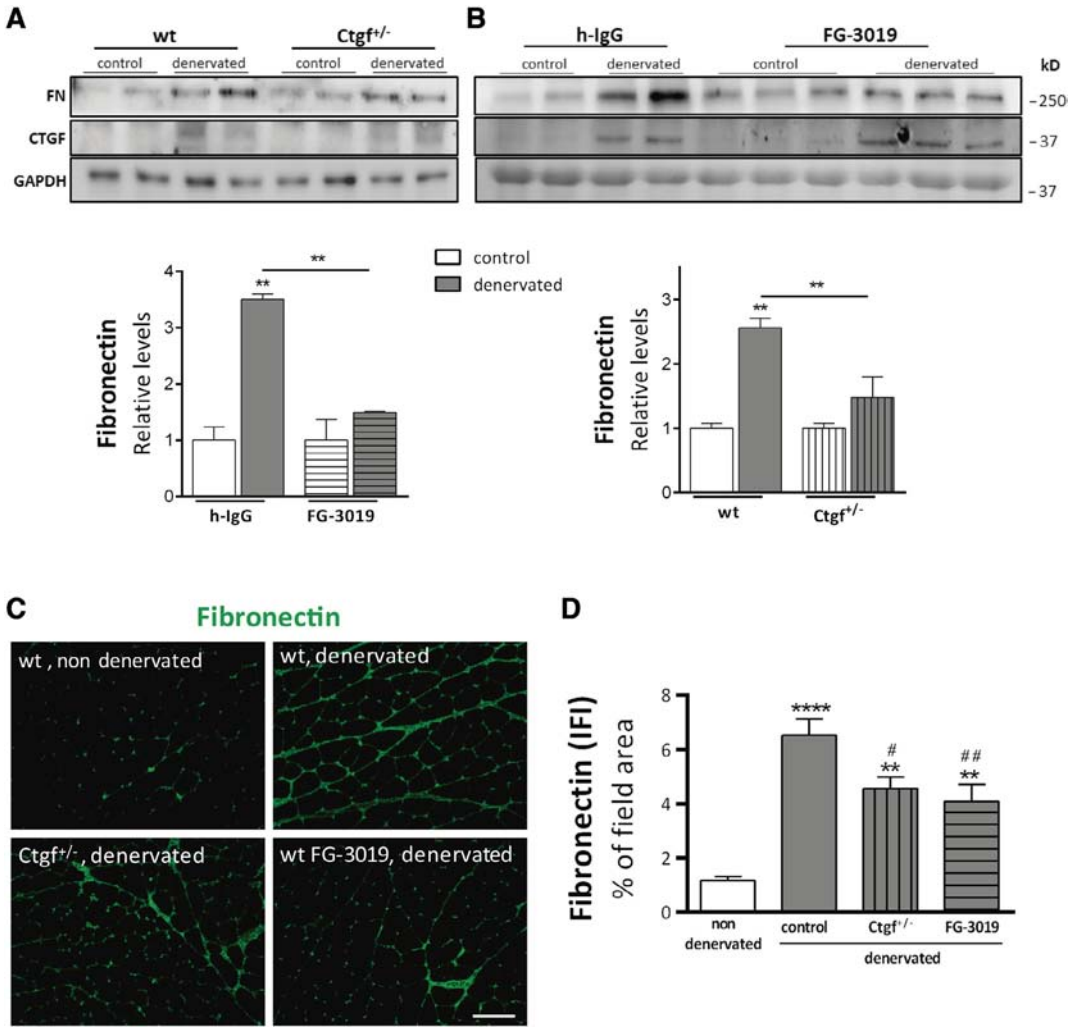

Fig. 7. Mice with decreased CTGF levels or activity present less skeletal muscle ECM accumulation 4 days after denervation. Mice that are hemizygous for CTGF (A), and mice treated with the CTGF-blocking antibody (FG-3019) (B), and their controls (C57BL10 and C57BL10 treated with h-IgG, respectively), were subjected to unilateral sciatic denervation and skeletal muscle from both hindlimbs collected 4 days after denervation. Muscle homogenates were analyzed by WB for detection of fibronectin and CTGF. Densitometric analysis is shown below each representative WB image. C. IFI against fibronectin in the same experimental conditions presented before. Ctgf$^{+/-}$ and FG-3019-treated mice exhibit less accumulation of ECM proteins at day 4 after denervation when compared to controls, which is quantified in D. Bar: 100 μm. Symbols: * comparing contralateral to denervated muscles; # comparing Ctgf$^{+/-}$ or FG-3019 denervated muscles to vehicle (*wt* or h-IgG) denervated muscles.

of full denervation, the loss of motoneuron communication increases skeletal muscle CTGF/CCN2 and fibrosis. However, bilateral denervation of the lower limbs is not able to induce CTGF/CCN2 expression in the spinal cord (Supplementary Fig. 5), suggesting that in the ALS model increased CTGF/CCN2 in skeletal muscle is a consequence of denervation, but augmented CTGF/CCN2 in the spinal cord is indeed due to overexpression of mutant SOD1 and the concomitant spinal cord degeneration [34].

Fibrosis was evaluated by an increase in total collagen, collagen type I and fibronectin. Previously, we have shown that proteoglycans are augmented in skeletal muscle after denervation [12,14] and in muscular dystrophies [63,64]. Several types of proteoglycans have been involved in skeletal muscle pathophysiology, either at the neuromuscular junction [65–67] or in the skeletal muscle surface [68]. Particularly attractive is decorin, a chondroitin/dermatan sulfate proteoglycan [69] that increases its expression after denervation [14]. Decorin has the ability to regulate the activity of TGF-β modulating skeletal muscle formation [68,70–72]. Its role during skeletal muscular diseases has been demonstrated [1]. Interestingly, decorin can inhibit TGF-β mediated action in response to skeletal muscle injury [73,74]

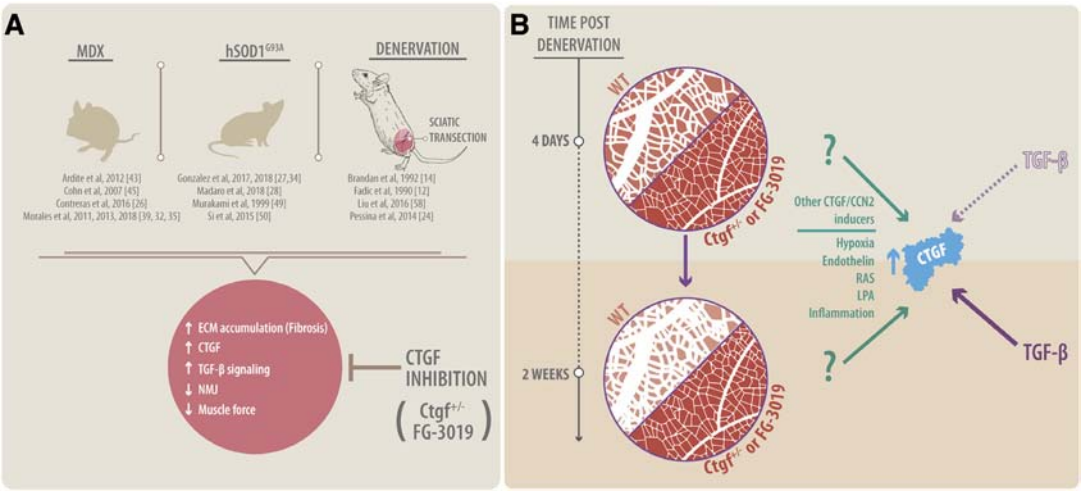

Fig. 8. CTGF/CCN2 participation in neuromuscular diseases. A. Detrimental CTGF/CCN2 role in the fibrotic phenotype of neuromuscular diseases murine models. B. Early CTGF/CCN2 participation in the fibrotic response after denervation is independent of TGF-β signaling.

and also interacts with CTGF/CCN2 inhibiting its action and regulating its biological activity [75]. Future experiments are required to understand the role of decorin or other proteoglycans modulating the activity of these pro-fibrotic factors and others in neuromuscular diseases.

Our results indicate that the increase in fibrosis, as consequence of denervation, seems to be at least dependent of two components, CTGF/CCN2 and TGF-β mediated signaling, acting at different times after nerve transection. Time course experiments showed that accumulation of CTGF/CCN2 and ECM proteins such as fibronectin and collagen I in the skeletal muscle rise very early after denervation, as soon as 2 days after sciatic nerve transection, while the activation of canonical TGF-β seems to be a later event. The kinetics of the fibrotic response after denervation, together with downregulation of TGF-β signaling (by inhibition of TGF-β-RI kinase or TGF-β release) suggest that in our model skeletal muscle CTGF/CCN2 is not up-regulated by canonical TGF-β signaling early after denervation (Fig. 8).

TGF-β is a strong CTGF/CCN2 inducer, but there are other factors that also regulate CTGF/CCN2 expression. In other fibrotic models such as skin scleroderma, renal and lung fibrosis, and systemic sclerosis, cell response to low oxygen pressure or hypoxia has been associated with up-regulation of CTGF/CCN2 and ECM proteins via mechanisms that can be independent of TGF-β [76–79]. Endothelin-1, a vasoconstrictor involved in cardiovascular disease, and its receptors have also been reported to induce CTGF/CCN2 and a subsequent fibrotic response in lung and skin fibrosis, systemic sclerosis and cardiac myocytes [80–83]. Angiotensin II, a vasoactive peptide of the renin-angiotensin system (RAS), can induce CTGF/CCN2 levels via mechanisms that can be dependent or independent of TGF-β [84,85]. Also, the action of bioactive lipids, such as lysophosphatidic acid (LPA), has been linked to fibrosis of different etiology [86–88] and our laboratory demonstrated that LPA is able to induce CTGF/CCN2 in muscle cells in vitro [75,89,90]. Inflammatory cytokines are known triggers of the fibrotic response. Although there is no significant infiltration of immune cells in denervated tissue, small inflammatory responses are observed with increases of IL-1β, IL-15 and TNF-α [91]. Furthermore, there is persistently activated STAT3-IL-6 signaling in denervated FAPs that can contribute to fibrosis and muscle atrophy after denervation [28]. Also, in mechanically stressed fibroblasts, the expression of CTGF/CCN2 precedes that of TGF-β [92]. Therefore, these and other factors that might be modulating the fibrotic response immediately after skeletal muscle denervation need to be studied in detail. The exploration of these factors might open new therapeutic alternatives for skeletal muscle wasting and fibrosis due to full denervation (e.g. from traumatic nerve injury) or pathological conditions in which progressive denervation occurs.

Experimental procedures

Animals, denervation protocol and tissue collection

All protocols were conducted in strict accordance and with formal approval of the Animal Ethics Committee of the Pontificia Universidad Católica de Chile. We used 6–7-month-old C57/BL10 wild type and CTGF/CCN2$^{+/-}$ males (in the same genetic background). The latter was kindly donated

by Professor Roel Goldschmeding (UMC, The Netherlands). For detection of FAPs, 6–7-month-old *Pdgfra*$^{tm11(EGFP)Sor}$ mice were used (JAX stock #007669) [51]. For denervation experiments, animals were anesthetized with 3.0% isoflurane gas in pure oxygen and a small incision (≤0.5 mm) is made in the left tight skin. Muscle packages from gluteal and biceps femoris muscles were carefully separated by cutting the facia. The sciatic nerve was exposed with the help of a small surgical hook and then cut before the separation of sciatic nerve branches [19,26]. A small (2–5 mm) section was removed to prevent reinnervation. Denervation was performed unilaterally, using the contralateral hindlimb as a control. 2, 4, 7 or 14 days after denervation surgery, mice were anesthetized with isoflurane and euthanized by cervical dislocation. GT muscles were dissected from denervated and contralateral hindlimbs. Muscle samples for cryosectioning were frozen in liquid nitrogen cooled-isopentane (Merck, Darmstadt, Germany) and stored at –80 °C until processing.

Treatment with the FG-3019 neutralizing antibody

Human monoclonal IgG antibody against CTGF/CCN2 (FG-3019) and non-specific h-IgG were obtained from FibroGen, Inc. 6–7-month-old wild type male mice were treated via intraperitoneal injection (IP). A dose of 25 mg/Kg was administered three times per week [32,34]. Denervation was performed 1 week after the treatment started. 4 days or 2 weeks after denervation, mice were euthanized as described above.

Treatment with TGF-βR kinase inhibitors

SB525334 and SB431542 were obtained from Sigma. A 10 mg/Kg dose was IP administered daily to 6–7-month-old wild type male mice. Denervation was performed 2 days after the first injection, and muscles were collected 4 days after denervation.

Treatment with SRI31277

SRI31277 peptide was synthesized by Biomatik USA (Wilmington, DE). Administration to 6–7-month-old wild type male mice was performed implanting a subcutaneous micro-osmotic pump (Alzet, model 1007D) delivering a 30 mg/Kg/day [53] dose during 7 days. The osmotic pump was implanted 3 days prior to denervation, and muscles were collected 4 days after denervation.

Isometric force measurement

Isolated TA muscle was submerged in a bath with a buffer containing oxygenated Krebs-Ringer solution. The knee bone and tendon were used to attach the muscle-to-muscle force transducer and the bottom of the bath respectively. The isometric force of isolated TA muscle was measured at optimum muscle length (L_o). Stimulation voltage was determined from the voltage necessary to produce a maximum isometric twitch force. Maximum isometric force was determined by stimulating from 1 to 200 Hz for 450 ms with 2 min rest between the stimuli. After measurements, the muscles were removed from the bath, trimmed of their tendons and of any non-muscle tissue and weighed. Specific force (force normalized with respect to muscle fiber cross-sectional area; mN/mm^2) was calculated from muscle mass and L_o [32,44].

Hematoxylin & eosin staining

GT muscle cryosections (7 µm) were placed onto glass slides. Hematoxylin and eosin (H&E) staining was performed to assess muscle architecture and histology. Briefly, tissue sections were incubated for 10 min in formalin (10% v/v), then washed with water, incubated for 5 min with diluted H&E (Merck, Darmstadt, Germany; 25% v/v in H_2O) and washed with water. Eosin was added for 30 s and then dehydration with ethanol was performed. Finally, Entellan (Merck, Darmstadt, Germany) was added to the slices. Sections were imaged using bright field microscopy on a Nikon Eclipse E600 [34].

Immunohistochemistry (IHC)

7 µm muscle cryosections were fixed in cold ethanol, rinsed in 0.05 M TBS buffer, pH 7.6, and incubated overnight with primary antibodies against CTGF/CCN2/CCN2 (sc-14939, Santa Cruz Biotechnology, Santa Cruz, CA, USA; (1:100 dilution in TCT buffer (TBS, carrageenan 0.7%, Triton X-100 0.25%)). Sections were placed at RT°, washed 3 times for 5 min in TBS and then incubated with secondary antibodies (1:100) for 30 min followed by three 5 min TBS washes. The sections were then incubated with peroxidase-anti-peroxidase (PAP) complex (1:200) (MP Biomedicals, Aurora, OH, USA) for 30 min, then washed in TBS 3 times for 5 min. The immunoperoxidase reaction was visualized after incubation of sections in 0.1% diaminobenzidine and 0.03% hydrogen peroxide for 2 min [36]. Sections were washed with tap water and counterstained with H&E, dehydrated in an ethanol gradient and cleared with xylene.

Indirect immunofluorescence (IFI)

For GT immunofluorescence, cryosections (7 µm) were fixed in 4% paraformaldehyde (Merck, Darmstadt, Germany), blocked for 1 h in blocking buffer (1% BSA, BM-0150, Winkler, Santiago, CL; 1% gelatin from cold water fish skin, G7765, Sigma, St. Louis, MO, USA; 0,01% Triton X-100, X100-1 L, Sigma, MO, St. Louis, USA) in PBS and incubated overnight at 4 °C with the following antibodies: anti-fibronectin (Sigma-

Aldrich, St. Louis, MO, USA), anti-collagen-I (Abcam, Cambridge, UK), anti-p-Smad3 (Cell Signaling, Danvers, MA, USA), anti-laminin (Sigma-Aldrich, St. Louis, MO, USA). The corresponding Alexa Fluor 568 or 488-conjugated anti-IgGs (Invitrogen, Carlsbad, CA, USA) were used as secondary antibodies. Alexa Fluor 594 conjugated-wheat germ agglutinin (WGA) (Thermo Fisher, Waltham, MA, USA) was used to stain cell surface. For nuclear staining, sections were incubated with 1 μg/mL Hoechst 33258 during the incubation with secondary antibodies. Slices were then washed in water and mounted in fluorescent mounting medium (DAKO, Santa Clara, CA, USA). For visualization of ECM proteins and pSmad3, cross-sections were visualized on a Nikon Eclipse E600 epifluorescence microscope with 20× or 40× objectives, using NIS-Elements software v4.20, 32 bit [26,27]. For evaluation of fiber versus interstitial nuclei for pSmad3 staining, cross-sections were imaged on a Nikon Eclipse C2 confocal spectral microscope using NIS-Elements AR software 4.00.00 (build 764) LO, 64 bit. The objective used was 40× Oil Plan Apo NA 1.0 WD 0.16 DIC H. a, b, x, y, images were zoomed 2.5× optically from the original picture.

Determination of occupied area and fiber diameter

For quantifying the area occupied by CTGF, collagen I or fibronectin, immunostained microphotographs from transversal muscle cryosections were selected by adjusting color threshold and measuring the area fraction with the ImageJ software (NIH, USA). Values were expressed as a percentage of area occupied or fold-change respect to contralateral muscle. For determination of fiber diameter, muscle cryosections stained for laminin or with fluorescent wheat germ agglutinin (WGA) were selected by adjusting color threshold and using the ROI manager plugin also from the ImageJ software and measuring the minimal Feret's diameter of each fiber [32]. Fiber size was calculated using individual or reconstructed images of the GT muscle. Quantifications were performed using 3–7 20× images per muscle, and 2–3 muscles per condition.

Immunoblot analysis

Skeletal muscles were homogenized in 10 volumes of Tris-EDTA buffer pH 7.4 with 1 mM phenylmethylsulfonyl fluoride (PMSF) using an Ultraturrax T25 (Labortechnik). Then, the same volume of buffer containing 2% glycerol, 4% SDS and 0.125 M Tris pH 6.8 was added to the homogenates and mixed. Muscle homogenates were incubated at 50 °C for 20 min and centrifuged for 10 min at 14,000 rpm to pellet insoluble material. Protein concentration in the supernatant was determined using the BCA Assay kit (Pierce, Rockford, IL, USA) with BSA as the standard. Aliquots (40–50 μg) were subjected to SDS-PAGE and transferred onto PVDF membranes (Millipore, Billerica, MA, USA). Membranes were blocked in 5% nonfat milk in TBS (50 mM Tris-Cl, pH 7.6; 150 mM NaCl) and probed with the following antibodies at 4 °C overnight: anti-fibronectin (Sigma-Aldrich, St. Louis, MO, USA), anti-pSmad3 (Cell Signaling, Danvers, MA, USA), anti-PDGFRα (R&D Systems, Minneapolis, MN, USA), anti-CTGF/CCN2 (Santa Cruz, USA), anti-GAPDH (Millipore, Billerica, MA, USA) and anti-α-tubulin (Sigma-Aldrich, St. Louis, MO, USA). Following incubation for 1 h at room temperature, primary antibodies were detected with horseradish-peroxidase-conjugated secondary antibodies. All immunoreactions were visualized by enhanced chemiluminescence (Pierce, Rockford, IL, USA). Densitometric analysis and quantification were performed using the ImageJ software (NIH, USA) [26,27].

RNA isolation, reverse transcription, and quantitative real-time PCR

Total RNA was isolated from GT muscle using TRIzol (Invitrogen) according to the manufacturer's recommendations. Total RNA (2 mg) was reverse transcribed into cDNA using random primers and M-MLV reverse transcriptase (Invitrogen). TaqMan quantitative real-time PCR reactions were performed in duplicate on an Eco Real-Time PCR System (Illumina, San Diego, CA, USA) using predesigned primer sets for mouse-TGFb1 gene (Mm01178820_m1) and the housekeeping gene GAPDH (Mm99999915_g1; TaqMan Assays-on-Demand, Applied Biosystems, Foster City, CA, USA). Alternatively, we used primer sets for mouse TGF-β1 (Fwd: 5′-CTCCACCTGCAAGACCAT-3′; Rev.: 5′-CTCCACCTGCAAGACCAT-3′) and for the housekeeping gene 18S (Fwd: 5′-TGACGGA AGGGCACCACCAG-3′; Rev.: 5′-CACCACCACC-CACGGAATCG-3′). mRNA expression was quantified with the comparative ΔCt method (2-ΔΔCt), using GAPDH as reference gene. The mRNA levels were expressed relative to the mean expression in control mice [26,27].

Statistical analyses

Data analyses and statistical analyses were performed using the Prism6 software (Graph Pad Software, CA, USA). Data are presented as Mean ± SEM. When only 2 groups were compared a paired *t*-test was performed to compare contralateral to denervated muscle. One-way ANOVA was used to evaluate more than two experimental groups. Newman-Keuls multiple comparison test was performed to compare differences between groups. p-Values: *$p \leq 0.05$; **$p \leq 0.01$; ***$p \leq 0.001$; ****$p \leq 0.0001$.

Supplementary data to this article can be found online at https://doi.org/10.1016/j.matbio.2019.01.002.

Acknowledgments

The authors are grateful to Eduardo Ramirez, Darling Vera, Lina Correa and Carlos Céspedes. for technical support. This work was supported by CONICYT AFB170005 and FONDECYT 1150106 to E.B.. FONDECYT Postdoctoral training grant 3140357 and Fondecyt 11181090 to D.L.R.. Beca de Doctorado Nacional Folio 21130854 and 21140378 to D.G. and O. C. respectively. J.E.M-U. was partially supported by funds from the Alabama Drug Discovery Alliance. The authors acknowledge the services provided by UC CINBIOT Animal Facility funded by PIA CONICYT* ECM-07, Program for Associative Research, of the Chilean National Council for Science and Technology. The funding agencies had no role in the design of the study, data collection, and analysis, the decision to publish, or preparation of the manuscript.

Received 26 October 2018;
Received in revised form 31 January 2019;
Accepted 31 January 2019
Available online 1 February 2019

Keywords:
Denervation;
Fibrosis;
CTGF/CCN2;
Skeletal muscle;
FG-3019

Abbreviations used:
ALS, Amyotrophic Lateral Sclerosis; CTGF/CCN2, connective tissue growth factor; ECM, extracellular matrix; FAPs, fibro/adipogenic progenitors; GT, gastrocnemius; H&E, Hematoxylin and eosin; h-IgG, Human immunoglobulin G; IFI, indirect immunofluorescence; IHC, immunohistochemistry; RAS, renin-angiotensin system; SOD1, Superoxide dismutase 1; TA, tibialis anterior; TGF-β, transforming growth factor type-β.

References

[1] E. Brandan, J. Gutierrez, Role of proteoglycans in the regulation of the skeletal muscle fibrotic response, FEBS J. 280 (17) (2013) 4109–4117.
[2] A.L. Serrano, P. Munoz-Canoves, Fibrosis development in early-onset muscular dystrophies: mechanisms and translational implications, Semin. Cell Dev. Biol. 64 (2017) 181–190.
[3] N.K. Karamanos, A.D. Theocharis, T. Neill, R.V. Iozzo, Matrix modeling and remodeling: a biological interplay regulating tissue homeostasis and diseases, Matrix Biol. (2018). https://doi.org/10.1016/j.matbio.2018.08.007.
[4] T.A. Wynn, T.R. Ramalingam, Mechanisms of fibrosis: therapeutic translation for fibrotic disease, Nat. Med. 18 (7) (2012) 1028–1040.
[5] A.L. Serrano, C.J. Mann, B. Vidal, E. Ardite, E. Perdiguero, P. Munoz-Canoves, Cellular and molecular mechanisms regulating fibrosis in skeletal muscle repair and disease, Curr. Top. Dev. Biol. 96 (2011) 167–201.
[6] A.L. Serrano, P. Munoz-Canoves, Regulation and dysregulation of fibrosis in skeletal muscle, Exp. Cell Res. 316 (18) (2010) 3050–3058.
[7] C. Gargioli, M. Coletta, F. De Grandis, S.M. Cannata, G. Cossu, PlGF-MMP-9-expressing cells restore microcirculation and efficacy of cell therapy in aged dystrophic muscle, Nat. Med. 14 (9) (2008) 973–978.
[8] L.R. Smith, E.R. Barton, Regulation of fibrosis in muscular dystrophy, Matrix Biol. 68-69 (2018) 602–615.
[9] P. Pasinelli, R.H. Brown, Molecular biology of amyotrophic lateral sclerosis: insights from genetics, Nat. Rev. Neurosci. 7 (9) (2006) 710–723.
[10] B.R. Thanvi, T.C. Lo, Update on myasthenia gravis, Postgrad. Med. J. 80 (950) (2004) 690–700.
[11] S.L. Rowan, K. Rygiel, F.M. Purves-Smith, N.M. Solbak, D.M. Turnbull, R.T. Hepple, Denervation causes fiber atrophy and myosin heavy chain co-expression in senescent skeletal muscle, PLoS One 7 (1) (2012), e29082.
[12] R. Fadic, E. Brandan, N.C. Inestrosa, Motor nerve regulates muscle extracellular matrix proteoglycan expression, J. Neurosci. 10 (11) (1990) 3516–3523.
[13] G. Ugarte, E. Brandan, Transforming growth factor beta (TGF-beta) signaling is regulated by electrical activity in skeletal muscle cells. TGF-beta type I receptor is transcriptionally regulated by myotube excitability, J. Biol. Chem. 281 (27) (2006) 18473–18481.
[14] E. Brandan, M.E. Fuentes, W. Andrade, Decorin, a chondroitin/dermatan sulfate proteoglycan is under neural control in rat skeletal muscle, J. Neurosci. Res. 32 (1) (1992) 51–59.
[15] M. Midrio, The denervated muscle: facts and hypotheses. A historical review, Eur. J. Appl. Physiol. 98 (1) (2006) 1–21.
[16] X. Yang, P. Xue, X. Liu, X. Xu, Z. Chen, HMGB1/autophagy pathway mediates the atrophic effect of TGF-beta1 in denervated skeletal muscle, Cell Commun. Signal 16 (1) (2018) 97.
[17] M.T. Kampman, S.L. Benestad, T. Fladby, J. Maehlen, Denervation enhances spontaneous inflammatory myopathy in SJL mice, Muscle Nerve 22 (7) (1999) 883–888.
[18] R. Xu, M.M. Salpeter, Acetylcholine receptors in innervated muscles of dystrophic mdx mice degrade as after denervation, J. Neurosci. 17 (21) (1997) 8194–8200.
[19] J. Batt, J. Bain, J. Goncalves, B. Michalski, P. Plant, M. Fahnestock, J. Woodgett, Differential gene expression profiling of short and long term denervated muscle, FASEB J. 20 (1) (2006) 115–117.
[20] S. Iqbal, O. Ostojic, K. Singh, A.M. Joseph, D.A. Hood, Expression of mitochondrial fission and fusion regulatory proteins in skeletal muscle during chronic use and disuse, Muscle Nerve 48 (6) (2013) 963–970.
[21] N. Suzuki, N. Motohashi, A. Uezumi, S. Fukada, T. Yoshimura, Y. Itoyama, M. Aoki, Y. Miyagoe-Suzuki, S. Takeda, NO production results in suspension-induced muscle atrophy through dislocation of neuronal NOS, J. Clin. Invest. 117 (9) (2007) 2468–2476.
[22] T.Y. Kostrominova, P.C. Macpherson, B.M. Carlson, D. Goldman, Regulation of myogenin protein expression in denervated muscles from young and old rats, Am. J. Phys. Regul. Integr. Comp. Phys. 279 (1) (2000) R179–R188.
[23] Y. Mochizuki, K. Ojima, A. Uezumi, S. Masuda, K. Yoshimura, S. Takeda, Participation of bone marrow-derived cells in fibrotic

changes in denervated skeletal muscle, Am. J. Pathol. 166 (6) (2005) 1721–1732.
[24] P. Pessina, D. Cabrera, M.G. Morales, C.A. Riquelme, J. Gutierrez, A.L. Serrano, E. Brandan, P. Munoz-Canoves, Novel and optimized strategies for inducing fibrosis in vivo: focus on Duchenne Muscular Dystrophy, Skelet. Muscle 4 (2014) 7.
[25] S. Caceres, C. Cuellar, J.C. Casar, J. Garrido, L. Schaefer, H. Kresse, E. Brandan, Synthesis of proteoglycans is augmented in dystrophic mdx mouse skeletal muscle, Eur. J. Cell Biol. 79 (3) (2000) 173–181.
[26] O. Contreras, D.L. Rebolledo, J.E. Oyarzun, H.C. Olguin, E. Brandan, Connective tissue cells expressing fibro/adipogenic progenitor markers increase under chronic damage: relevance in fibroblast-myofibroblast differentiation and skeletal muscle fibrosis, Cell Tissue Res. 364 (3) (2016) 647–660.
[27] D. Gonzalez, O. Contreras, D.L. Rebolledo, J.P. Espinoza, B. van Zundert, E. Brandan, ALS skeletal muscle shows enhanced TGF-beta signaling, fibrosis and induction of fibro/adipogenic progenitor markers, PLoS One 12 (5) (2017), e0177649.
[28] L. Madaro, M. Passafaro, D. Sala, U. Etxaniz, F. Lugarini, D. Proietti, M.V. Alfonsi, C. Nicoletti, S. Gatto, M. De Bardi, R. Rojas-Garcia, L. Giordani, S. Marinelli, V. Pagliarini, C. Sette, A. Sacco, P.L. Puri, Denervation-activated STAT3-IL-6 signalling in fibro-adipogenic progenitors promotes myofibres atrophy and fibrosis, Nat. Cell Biol. 20 (8) (2018) 917–927.
[29] A. Leask, Signaling in fibrosis: targeting the TGF beta, endothelin-1 and CCN2 axis in scleroderma, Front. Biosci. (Elite Ed.) 1 (2009) 115–122.
[30] Y. Ito, J. Aten, T.Q. Nguyen, J.A. Joles, S. Matsuo, J.J. Weening, R. Goldschmeding, Involvement of connective tissue growth factor in human and experimental hypertensive nephrosclerosis, Nephron Exp. Nephrol. 117 (1) (2011) e9–20.
[31] G. Sun, K. Haginoya, Y. Wu, Y. Chiba, T. Nakanishi, A. Onuma, Y. Sato, M. Takigawa, K. Iinuma, S. Tsuchiya, Connective tissue growth factor is overexpressed in muscles of human muscular dystrophy, J. Neurol. Sci. 267 (1–2) (2008) 48–56.
[32] M.G. Morales, J. Gutierrez, C. Cabello-Verrugio, D. Cabrera, K. E. Lipson, R. Goldschmeding, E. Brandan, Reducing CTGF/CCN2 slows down mdx muscle dystrophy and improves cell therapy, Hum. Mol. Genet. 22 (24) (2013) 4938–4951.
[33] C.G. Au, T.L. Butler, M.C. Sherwood, J.R. Egan, K.N. North, D. S. Winlaw, Increased connective tissue growth factor associated with cardiac fibrosis in the mdx mouse model of dystrophic cardiomyopathy, Int. J. Exp. Pathol. 92 (1) (2011) 57–65.
[34] D. Gonzalez, D.L. Rebolledo, L.M. Correa, F.A. Court, W. Cerpa, K.E. Lipson, B. van Zundert, E. Brandan, The inhibition of CTGF/CCN2 activity improves muscle and locomotor function in a murine ALS model, Hum. Mol. Genet. 27 (2018) 2913–2926.
[35] M.G. Morales, M.J. Acuna, D. Cabrera, R. Goldschmeding, E. Brandan, The pro-fibrotic connective tissue growth factor (CTGF/CCN2) correlates with the number of necrotic-regenerative foci in dystrophic muscle, J. Cell Commun. Signal 12 (1) (2018) 413–421.
[36] M.J. Acuña, D. Salas, A. Cordova-Casanova, M. Cruz-Soca, C. Cespedes, C.P. Vio, E. Brandan, Blockade of Bradykinin receptors worsens the dystrophic phenotype of mdx mice: differential effects for B1 and B2 receptors, J. Cell Commun. Signal 12 (2017) 589–601.
[37] A. Leask, D.J. Abraham, All in the CCN family: essential matricellular signaling modulators emerge from the bunker, J. Cell Sci. 119 (Pt 23) (2006) 4803–4810.
[38] X. Shi-Wen, A. Leask, D. Abraham, Regulation and function of connective tissue growth factor/CCN2 in tissue repair, scarring and fibrosis, Cytokine Growth Factor Rev. 19 (2) (2008) 133–144.
[39] M.G. Morales, C. Cabello-Verrugio, C. Santander, D. Cabrera, R. Goldschmeding, E. Brandan, CTGF/CCN-2 over-expression can directly induce features of skeletal muscle dystrophy, J. Pathol. 225 (4) (2011) 490–501.
[40] C. Vial, L.M. Zuniga, C. Cabello-Verrugio, P. Canon, R. Fadic, E. Brandan, Skeletal muscle cells express the profibrotic cytokine connective tissue growth factor (CTGF/CCN2), which induces their dedifferentiation, J. Cell. Physiol. 215 (2) (2008) 410–421.
[41] A. Leask, D.J. Abraham, TGF-beta signaling and the fibrotic response, FASEB J. 18 (7) (2004) 816–827.
[42] T.A. Wynn, Cellular and molecular mechanisms of fibrosis, J. Pathol. 214 (2) (2008) 199–210.
[43] E. Ardite, E. Perdiguero, B. Vidal, S. Gutarra, A.L. Serrano, P. Munoz-Canoves, PAI-1-regulated miR-21 defines a novel age-associated fibrogenic pathway in muscular dystrophy, J. Cell Biol. 196 (1) (2012) 163–175.
[44] M.J. Acuña, P. Pessina, H. Olguin, D. Cabrera, C.P. Vio, M. Bader, P. Munoz-Canoves, R.A. Santos, C. Cabello-Verrugio, E. Brandan, Restoration of muscle strength in dystrophic muscle by angiotensin-1-7 through inhibition of TGF-beta signalling, Hum. Mol. Genet. 23 (5) (2014) 1237–1249.
[45] R.D. Cohn, C. van Erp, J.P. Habashi, A.A. Soleimani, E.C. Klein, M.T. Lisi, M. Gamradt, C.M. ap Rhys, T.M. Holm, B.L. Loeys, F. Ramirez, D.P. Judge, C.W. Ward, H.C. Dietz, Angiotensin II type 1 receptor blockade attenuates TGF-beta-induced failure of muscle regeneration in multiple myopathic states, Nat. Med. 13 (2) (2007) 204–210.
[46] J. Massague, TGF-beta signal transduction, Annu. Rev. Biochem. 67 (1998) 753–791.
[47] J.G. Abreu, N.I. Ketpura, B. Reversade, E.M. De Robertis, Connective-tissue growth factor (CTGF) modulates cell signalling by BMP and TGF-beta, Nat. Cell Biol. 4 (8) (2002) 599–604.
[48] T. Mori, S. Kawara, M. Shinozaki, N. Hayashi, T. Kakinuma, A. Igarashi, M. Takigawa, T. Nakanishi, K. Takehara, Role and interaction of connective tissue growth factor with transforming growth factor-beta in persistent fibrosis: a mouse fibrosis model, J. Cell. Physiol. 181 (1) (1999) 153–159.
[49] N. Murakami, I.S. McLennan, I. Nonaka, K. Koishi, C. Baker, G. Hammond-Tooke, Transforming growth factor-beta2 is elevated in skeletal muscle disorders, Muscle Nerve 22 (7) (1999) 889–898.
[50] Y. Si, S. Kim, X. Cui, L. Zheng, S.J. Oh, T. Anderson, M. AlSharabati, M. Kazamel, L. Volpicelli-Daley, M.M. Bamman, S. Yu, P.H. King, Transforming growth factor beta (TGF-beta) is a muscle biomarker of disease progression in ALS and correlates with Smad expression, PLoS One 10 (9) (2015), e0138425.
[51] T.G. Hamilton, R.A. Klinghoffer, P.D. Corrin, P. Soriano, Evolutionary divergence of platelet-derived growth factor alpha receptor signaling mechanisms, Mol. Cell. Biol. 23 (11) (2003) 4013–4025.
[52] S. Ivkovic, B.S. Yoon, S.N. Popoff, F.F. Safadi, D.E. Libuda, R.C. Stephenson, A. Daluiski, K.M. Lyons, Connective tissue growth factor coordinates chondrogenesis and angiogenesis during skeletal development, Development 130 (12) (2003) 2779–2791.
[53] A. Lu, M.A. Pallero, W. Lei, H. Hong, Y. Yang, M.J. Suto, J.E. Murphy-Ullrich, Inhibition of transforming growth factor-beta

activation diminishes tumor progression and osteolytic bone disease in mouse models of multiple myeloma, Am. J. Pathol. 186 (3) (2016) 678–690.
[54] K. Bailey Dubose, M. Zayzafoon, J.E. Murphy-Ullrich, Thrombospondin-1 inhibits osteogenic differentiation of human mesenchymal stem cells through latent TGF-beta activation, Biochem. Biophys. Res. Commun. 422 (3) (2012) 488–493.
[55] Y. Zhou, M.H. Poczatek, K.H. Berecek, J.E. Murphy-Ullrich, Thrombospondin 1 mediates angiotensin II induction of TGF-beta activation by cardiac and renal cells under both high and low glucose conditions, Biochem. Biophys. Res. Commun. 339 (2) (2006) 633–641.
[56] J.E. Nor, L. Dipietro, J.E. Murphy-Ullrich, R.O. Hynes, J. Lawler, P.J. Polverini, Activation of latent TGF-beta1 by thrombospondin-1 is a major component of wound repair, Oral. Biosci. Med. 2 (2) (2005) 153–161.
[57] J.E. Murphy-Ullrich, M.J. Suto, Thrombospondin-1 regulation of latent TGF-beta activation: a therapeutic target for fibrotic disease, Matrix Biol. 68-69 (2018) 28–43.
[58] F. Liu, W. Tang, D. Chen, M. Li, Y. Gao, H. Zheng, S. Chen, Expression of TGF-beta1 and CTGF is associated with fibrosis of denervated sternocleidomastoid muscles in mice, Tohoku J. Exp. Med. 238 (1) (2016) 49–56.
[59] J. Ozawa, T. Kurose, S. Kawamata, A. Kaneguchi, H. Moriyama, N. Kito, Regulation of connective tissue remodeling in the early phase of denervation in a rat skeletal muscle, Biomed. Res. 34 (5) (2013) 251–258.
[60] P. Mary, L. Servais, R. Vialle, Neuromuscular diseases: diagnosis and management, Orthop. Traumatol. Surg. Res. 104 (1S) (2018) S89–S95.
[61] D. Cabrera, J. Gutierrez, C. Cabello-Verrugio, M.G. Morales, S. Mezzano, R. Fadic, J.C. Casar, J.L. Hancke, E. Brandan, Andrographolide attenuates skeletal muscle dystrophy in mdx mice and increases efficiency of cell therapy by reducing fibrosis, Skelet. Muscle 4 (2014) 6.
[62] T. Tando, A. Hirayama, M. Furukawa, Y. Sato, T. Kobayashi, A. Funayama, A. Kanaji, W. Hao, R. Watanabe, M. Morita, T. Oike, K. Miyamoto, T. Soga, M. Nomura, A. Yoshimura, M. Tomita, M. Matsumoto, M. Nakamura, Y. Toyama, T. Miyamoto, Smad2/3 proteins are required for immobilization-induced skeletal muscle atrophy, J. Biol. Chem. 291 (23) (2016) 12184–12194.
[63] K. Alvarez, R. Fadic, E. Brandan, Augmented synthesis and differential localization of heparan sulfate proteoglycans in Duchenne muscular dystrophy, J. Cell. Biochem. 85 (4) (2002) 703–713.
[64] R. Fadic, V. Mezzano, K. Alvarez, D. Cabrera, J. Holmgren, E. Brandan, Increase in decorin and biglycan in Duchenne Muscular Dystrophy: role of fibroblasts as cell source of these proteoglycans in the disease, J. Cell. Mol. Med. 10 (3) (2006) 758–769.
[65] J.R. Sanes, M. Schachner, J. Covault, Expression of several adhesive macromolecules (N-CAM, L1, J1, NILE, uvomorulin, laminin, fibronectin, and a heparan sulfate proteoglycan) in embryonic, adult, and denervated adult skeletal muscle, J. Cell Biol. 102 (2) (1986) 420–431.
[66] C.L. Gatchalian, M. Schachner, J.R. Sanes, Fibroblasts that proliferate near denervated synaptic sites in skeletal muscle synthesize the adhesive molecules tenascin(J1), N-CAM, fibronectin, and a heparan sulfate proteoglycan, J. Cell Biol. 108 (5) (1989) 1873–1890.
[67] M.A. Samuel, G. Valdez, J.C. Tapia, J.W. Lichtman, J.R. Sanes, Agrin and synaptic laminin are required to maintain adult neuromuscular junctions, PLoS One 7 (10) (2012), e46663.
[68] E. Brandan, J. Gutierrez, Role of skeletal muscle proteoglycans during myogenesis, Matrix Biol. 32 (6) (2013) 289–297.
[69] T. Neill, L. Schaefer, R.V. Iozzo, Decorin: a guardian from the matrix, Am. J. Pathol. 181 (2) (2012) 380–387.
[70] C. Riquelme, J. Larrain, E. Schonherr, J.P. Henriquez, H. Kresse, E. Brandan, Antisense inhibition of decorin expression in myoblasts decreases cell responsiveness to transforming growth factor beta and accelerates skeletal muscle differentiation, J. Biol. Chem. 276 (5) (2001) 3589–3596.
[71] H.C. Olguin, C. Santander, E. Brandan, Inhibition of myoblast migration via decorin expression is critical for normal skeletal muscle differentiation, Dev. Biol. 259 (2) (2003) 209–224.
[72] R. Droguett, C. Cabello-Verrugio, C. Riquelme, E. Brandan, Extracellular proteoglycans modify TGF-beta bio-availability attenuating its signaling during skeletal muscle differentiation, Matrix Biol. 25 (6) (2006) 332–341.
[73] C. Cabello-Verrugio, E. Brandan, A novel modulatory mechanism of transforming growth factor-beta signaling through decorin and LRP-1, J. Biol. Chem. 282 (26) (2007) 18842–18850.
[74] C. Cabello-Verrugio, C. Santander, C. Cofre, M.J. Acuna, F. Melo, E. Brandan, The internal region leucine-rich repeat 6 of decorin interacts with low density lipoprotein receptor-related protein-1, modulates transforming growth factor (TGF)-beta-dependent signaling, and inhibits TGF-beta-dependent fibrotic response in skeletal muscles, J. Biol. Chem. 287 (9) (2012) 6773–6787.
[75] C. Vial, J. Gutierrez, C. Santander, D. Cabrera, E. Brandan, Decorin interacts with connective tissue growth factor (CTGF)/CCN2 by LRR12 inhibiting its biological activity, J. Biol. Chem. 286 (27) (2011) 24242–24252.
[76] D.F. Higgins, M.P. Biju, Y. Akai, A. Wutz, R.S. Johnson, V.H. Haase, Hypoxic induction of Ctgf is directly mediated by Hif-1, Am. J. Physiol. Ren. Physiol. 287 (6) (2004) F1223–F1232.
[77] Y.K. Lee, E.J. Kim, J.E. Lee, J.W. Noh, Y.G. Kim, Hypoxia induces connective tissue growth factor mRNA expression, J. Korean Med. Sci. (Suppl. 24) (2009) S176–S182.
[78] K.H. Hong, S.A. Yoo, S.S. Kang, J.J. Choi, W.U. Kim, C.S. Cho, Hypoxia induces expression of connective tissue growth factor in scleroderma skin fibroblasts, Clin. Exp. Immunol. 146 (2) (2006) 362–370.
[79] J.H. Distler, A. Jungel, M. Pileckyte, J. Zwerina, B.A. Michel, R.E. Gay, O. Kowal-Bielecka, M. Matucci-Cerinic, G. Schett, H.H. Marti, S. Gay, O. Distler, Hypoxia-induced increase in the production of extracellular matrix proteins in systemic sclerosis, Arthritis Rheum. 56 (12) (2007) 4203–4215.
[80] C.M. Weng, C.C. Yu, M.L. Kuo, B.C. Chen, C.H. Lin, Endothelin-1 induces connective tissue growth factor expression in human lung fibroblasts by ETAR-dependent JNK/AP-1 pathway, Biochem. Pharmacol. 88 (3) (2014) 402–411.
[81] J. Jing, T.T. Dou, J.Q. Yang, X.B. Chen, H.L. Cao, M. Min, S.Q. Cai, M. Zheng, X.Y. Man, Role of endothelin-1 in the skin fibrosis of systemic sclerosis, Eur. Cytokine Netw. 26 (1) (2015) 10–14.
[82] C.M. Weng, B.C. Chen, C.H. Wang, P.H. Feng, M.J. Lee, C.D. Huang, H.P. Kuo, C.H. Lin, The endothelin A receptor mediates fibrocyte differentiation in chronic obstructive asthma. The involvement of connective tissue growth factor, Am. J. Respir. Crit. Care Med. 188 (3) (2013) 298–308.
[83] A.G. Recchia, E. Filice, D. Pellegrino, A. Dobrina, M.C. Cerra, M. Maggiolini, Endothelin-1 induces connective tissue growth factor expression in cardiomyocytes, J. Mol. Cell. Cardiol. 46 (3) (2009) 352–359.

[84] C.K.S. Wong, A. Falkenham, T. Myers, J.F. Legare, Connective tissue growth factor expression after angiotensin II exposure is dependent on transforming growth factor-beta signaling via the canonical Smad-dependent pathway in hypertensive induced myocardial fibrosis, J. Renin-Angiotensin-Aldosterone Syst. 19 (1) (2018) (1470320318759358).

[85] A. Li, J. Zhang, X. Zhang, J. Wang, S. Wang, X. Xiao, R. Wang, P. Li, Y. Wang, Angiotensin II induces connective tissue growth factor expression in human hepatic stellate cells by a transforming growth factor beta-independent mechanism, Sci. Rep. 7 (1) (2017) 7841.

[86] H. Ikeda, Y. Yatomi, M. Yanase, H. Satoh, A. Nishihara, M. Kawabata, K. Fujiwara, Effects of lysophosphatidic acid on proliferation of stellate cells and hepatocytes in culture, Biochem. Biophys. Res. Commun. 248 (2) (1998) 436–440.

[87] N. Watanabe, H. Ikeda, K. Nakamura, R. Ohkawa, Y. Kume, J. Aoki, K. Hama, S. Okudaira, M. Tanaka, T. Tomiya, M. Yanase, K. Tejima, T. Nishikawa, M. Arai, H. Arai, M. Omata, K. Fujiwara, Y. Yatomi, Both plasma lysophosphatidic acid and serum autotaxin levels are increased in chronic hepatitis C, J. Clin. Gastroenterol. 41 (6) (2007) 616–623.

[88] A.M. Tager, P. LaCamera, B.S. Shea, G.S. Campanella, M. Selman, Z. Zhao, V. Polosukhin, J. Wain, B.A. Karimi-Shah, N.D. Kim, W.K. Hart, A. Pardo, T.S. Blackwell, Y. Xu, J. Chun, A.D. Luster, The lysophosphatidic acid receptor LPA1 links pulmonary fibrosis to lung injury by mediating fibroblast recruitment and vascular leak, Nat. Med. 14 (1) (2008) 45–54.

[89] C. Cabello-Verrugio, G. Cordova, C. Vial, L.M. Zuniga, E. Brandan, Connective tissue growth factor induction by lysophosphatidic acid requires transactivation of transforming growth factor type beta receptors and the JNK pathway, Cell. Signal. 23 (2) (2011) 449–457.

[90] C. Riquelme-Guzman, O. Contreras, E. Brandan, Expression of CTGF/CCN2 in response to LPA is stimulated by fibrotic extracellular matrix via the integrin/FAK axis, Am. J. Phys. Cell Physiol. 314 (4) (2018) C415–C427.

[91] H. Hanwei, H. Zhao, FYN-dependent muscle-immune interaction after sciatic nerve injury, Muscle Nerve 42 (1) (2010) 70–77.

[92] D. Kessler, S. Dethlefsen, I. Haase, M. Plomann, F. Hirche, T. Krieg, B. Eckes, Fibroblasts in mechanically stressed collagen lattices assume a “synthetic” phenotype, J. Biol. Chem. 276 (39) (2001) 36575–36585.